INTELEC 09 - 31st International Telecommunications Energy Conference

October 18-22, 2009, Songdo Convensia, Incheon, Korea

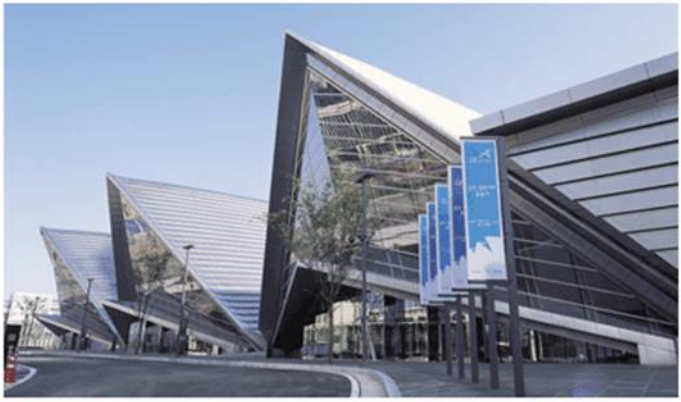

Organized by

KIEE(The Korean Institute of Electrical Engineers)

Technical Co-sponsorship

IEEE PELS (IEEE Power Electronic Society)

IEICE (The Institute of Electronics, Information and Communication Engineers)

IEEJ (The Institute of Electrical Engineers of Japan)

KIPE (The Korean Institute of Power Electronics)

Electric Machine and Drives (Poster Presentation) Oct, 21, 2009 (Wed,) 10:30-12:00

10:30-12:00 · PEM-1
Re-acceleration Characteristics of Stationary Discontinuous Armature Permanent Magnet Linear Synchronous Motor by Using Each Control System
Yong-Jae Kim, Kyoung-Pil Cho, Seung-Ho Shin, Youn-Ok Choi, Geum-Bae Cho (Chosun University, Korea)

10:30-12:00 · PEM-2
Development of IPM Synchronous Motor for Diesel Hybrid Electric Vehicle
Ju-Hee Cho, Hong-Seok Oh, Sang-Uk Cho, Deok-Geun-Kim (Komotek Co,. Ltd, Korea), Ik-Seong Park (LIGNex1 Co,. Ltd, Korea)

10:30-12:00 · PEM-3
The Velocity Control of a Permanent Magnet Type Stepping Motor Using a Self-tuning Theory
Sung-Ho Hong, Soo-Rang Lee, Sung-Hwan Choi (R&D Center CU Medical Systems, Inc,, Korea), Young-Tae Kim, Sang-Don Lee (Kangnung Wonju National University, Korea), Cherl-Jin Kim (Halla University, Korea)

10:30-12:00 · PEM-4
Double-layer Rotor Design for Improving Characteristics of Single-phase LSPM Motor
Byeong-Hwa Lee, Fangliang, Jung-Pyo Hong (Hanyang University, Korea), Hyuk Nam (LG Electronics, Korea)

10:30-12:00 · PEM-5
Output Voltage Control of a Synchronous Generator for Ships Using Compound Type Digital AVR
Sang-Hoon Park, Seung-Kyung Lee, Su-Won Lee (Sungkyunkwan University, Korea), Jae-Sung Yu (HYOSUNG Heavy Industries Co,. Ltd,. Korea), Sang-Seuk Lee (PACTECH, Korea), Chung-Yuen Won (Sungkyunkwan University, Korea)

10:30-12:00 · PEM-6
Optimization of Magnetic Suspension Using Response Surface Methodology
Ho-Kyoung Lim, Jae-Woo Jung, Jung-Pyo Hong (Hanyang University, Korea)

10:30-12:00 · PEM-7
Novel Position Sensorless Starting Method of BLDC Motor for Reciprocating Compressor
Dae-Kyong Kim, Duck-Shik Shin (Korea Electronics Technology Institute, Korea), Sang-Taek Lee (Korea Electronics Technology Institute, Hanynag University, Korea), Hee-Jun Kim, Byung-Il Kwon (Hanynag University, Korea), Byung-Taek Kim (Kunsan National University, Korea), Kwang-Woon Lee (Mokpo National Maritime University, Korea)

10:30-12:00 · PEM-8
Optimal Design for Cogging Torque Reduction in BLDC Motor Using the Response Surface Method
Young-Kyoun Kim, Jung-Moo Seo, Seung-Bin Lim, Se-Hyun Rhyu, In-Sung Jung (Kore Electronics Technology Institute, Korea), Jin Hur (University of Ulsan, Korea)

10:30-12:00 · PEM-9
Core Loss Distribution of Three-Phase Induction Motor Using Numerical Method
Jeong-Jong Lee, Soon-O Kwon, Jung-Pyo Hong (Hanyang University, Korea), Ji-Hyun Kim, Kyung-Ho Ha (POSCO, Korea)

10:30-12:00 · PEM-10
Minimization of Torque Ripple in a BLDC Motor Using an Improved DC Link Voltage Control Method
Jin-soek Jang, Byung-taek Kim (Kunsan National University, Korea)

10:30-12:00
Finite Element Analysis of a Very Large-Scale Permanent Magnet BLDC Motor Considering Two-dimensional Magnetic Properties of Electrical Steels

Double-layer Rotor Design for Improving Characteristics of Single-phase LSPM Motor

Byeong-Hwa Lee[1], Fangliang[1,] Jung-Pyo Hong[1], Hyuk Nam[2]
[1]Dept. of Automotive Engineering, Hanyang University, Seoul 133-791, Korea
[2] LG Electronics, Changwon, Gyeongnam 641-711, Korea
lbhwa@hanyang.ac.kr, hongjp@hanyang.ac.kr

Abstract — This paper deals with double-layer rotor design and design method of a single-phase line-start permanent magnet (LSPM) motor considering the efficiency and maximum torque with d-and q-axis equivalent circuit and finite element method (FEM). The motor parameters meeting the required efficiency, starting and maximum torque are determined by the characteristic map obtained by the d-q axis equivalent circuit analysis, then the geometric shape design satisfying the motor parameters are performed with FEM. In the end, the improved double-layer LSPM motor is fabricated and tested in order to measure the efficiency and maximum torque.

I. INTRODUCTION

A single-phase induction motor operating with commercial electricity without power electronic switching devices and position sensor is more economical and has higher maintenance than other inverter fed electrical motor [1]. So, it is becoming more generalized as direct operation by supplying the commercial single-phase voltage source of household appliance. However, the motor has problems such as the vibration caused due to unbalanced rotating field of main and subsidiary windings and the difficulty in improving efficiency because of the conductor bar loss [2].

Compared to the single-phase induction motor, a permanent magnet synchronous motor (PMSM) operating at synchronous speed with input frequency has high efficiency and compact size due to PM. However, the PMSM has problems such as high cogging torque and high cost due to PM, switching devices and rotor position sensor. Thus, a single-phase line-start permanent magnet (LSPM) motor complementing the single-phase induction motor and PMSM has been presented. The single-phase LSPM motor is essentially an induction motor added with PM material in rotor part. With the help of PM, efficiency at steady state is increased, but the maximum torque and starting torque, which consists of asynchronous cage torque and magnet braking torque, are decreased [3].

This paper presents a method to improve the efficiency and maximum torque of single-phase LSPM motor through double-layer rotor design using characteristic map obtained by d-and q-axis equivalent circuit analysis. The map indicates the direction of saliency ratio and back-EMF improving the efficiency and maximum torque. And then the prototype single-layer LSPM motor is optimized as improved double-layer LSPM motor satisfying the given efficiency and maximum torque through design of experiment (DOE) and response surface methodology (RSM). Finally, the characteristic analysis results of improved LSPM motor are compared to those of single-phase induction motor and prototype LSPM motor. Moreover, the improved LSPM motor is fabricated, and the efficiency and maximum torque of the motor are measured by test.

II. CHARACTERISTIC ANALYSIS OF SINGLE-PHASE LSPM MOTOR

The configuration and winding connection of a single-phase induction motor and prototype LSPM motor are shown in Fig. 1(a), (b), and (c) respectively. As shown in Fig. 1, both consist of main and subsidiary windings in the stator and conductor bars to produce the starting torque in the rotor. Starting capacitance Cs, running capacitance Cr, and positive temperature coefficient (PTC) are connected with the subsidiary windings to increase the starting torque and power factor. Accordingly, it could be considered as a two-phase motor.

A. Characteristic analysis method of Steady-state

A single-phase induction motor has the unbalanced rotating field due to main and subsidiary windings. The unbalanced field is considered by symmetrical coordinate method. So, the steady state analysis is performed by converting the single-phase LSPM motor into independently two balanced motors [4].

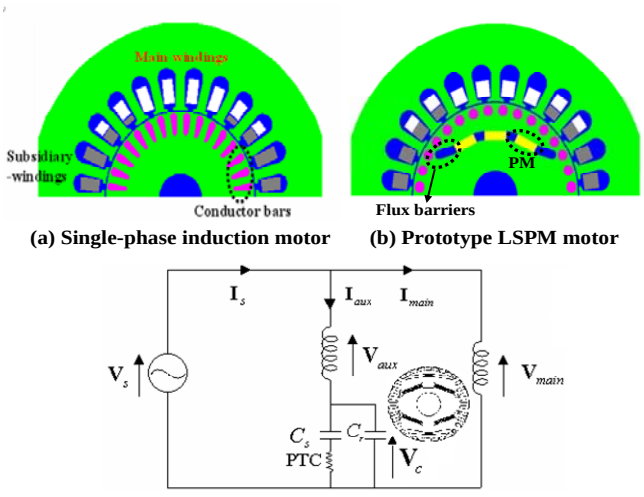

(a) Single-phase induction motor **(b) Prototype LSPM motor**

(c) Winding connection

Fig. 1. Single-phase induction motor, prototype LSPM motor and their stator winding connection

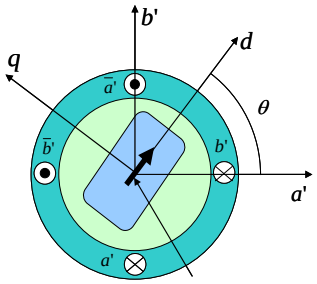

Fig. 2. D- and q-axis relation of stator winding and rotor in two-phase motor

1) Voltage equation

In the two-phase motor, d- and q-axis relation between stator winding and rotor is shown in Fig. 2. Form Fig. 2, stator voltage equation is as shown in (1).

$$\begin{bmatrix} v_d \\ v_q \end{bmatrix} = \begin{bmatrix} \cos\theta & \sin\theta \\ -\sin\theta & \cos\theta \end{bmatrix} \begin{bmatrix} v_a' \\ v_b' \end{bmatrix} \tag{1}$$

Where θ is electrical angle between magnemotive force axis of phase in the stator and d-axis in the rotor.

Also, d- and q-axis voltage equation of two-phase motor expressed as (2).

$$\begin{aligned} v_d &= (R_a' \cos^2\theta + R_b' \sin^2\theta) i_d + (-R_a' + R_b') \sin\theta\cos\theta i_q - X_q i_q \\ v_q &= (R_a' \sin^2\theta + R_b' \cos^2\theta) i_q + (-R_a' + R_b') \sin\theta\cos\theta i_d + X_d i_d + E \end{aligned} \tag{2}$$

From (2), the current of d- and q-axis is expressed as (3).

$$\begin{aligned} I_d &= \frac{-V_q(R_3 - X_q) + R_2 V_d + E(R_3 - X_q)}{R_1 R_2 - (R_3 + X_d)(R_3 - X_q)} \\ I_q &= \frac{-V_q(R_3 + X_q) + R_2 V_q - E R_1}{R_1 R_2 - (R_3 + X_d)(R_3 - X_q)} \end{aligned} \tag{3}$$

where $R_1' = R_a' \cos^2\theta + R_b' \sin^2\theta$; $R_2' = R_a' \sin^2\theta + R_b' \cos^2\theta$; $R_3' = (-R_a' + R_b') \sin\theta\cos\theta$.

2) Calculation of Characteristics

The symmetrical voltage and current components are calculated by the positive ad negative impedance, and then electrical power and mechanical torque composed of the positive and negative is written as (4).

$$\begin{aligned} P_1 &= (\mathrm{Re}(V_1 I_1^*) - R I_1^2) \longrightarrow T_1 = \frac{P_1}{\omega_s} \\ P_2 &= (\mathrm{Re}(V_2 I_2^*) - R I_2^2) \longrightarrow T_2 = \frac{P_2}{\omega_s} \\ T &= T_1 + T_2 \end{aligned} \tag{4}$$

3) Asynchronous characteristic analysis

A single-phase LSPM motor has both induction and synchronous motor characteristics according to the operating condition. The equivalent circuit for single-phase LSPM motor is shown in Fig. 3. Torque under non-synchronous condition is divided into cage torque and magnetic torque which are expressed as (5) and (6) respectively.

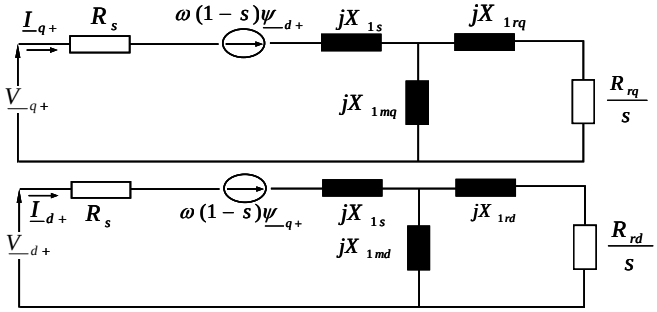

(a) Single-phase LSPM motor positive sequence circuit

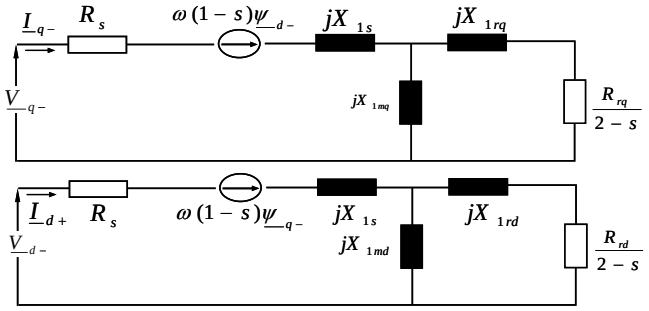

(b) Single-phase LSPM motor negative sequence circuit

Fig. 3. Single-phase LSPM motor equivalent circuit

The starting performances of LSPM motor is dominated by the magnet braking torque and changed according to the section area and shape of conductor bar, usage of PM and the capacity of capacitor.

$$\begin{aligned} T_{(cage)+} &= \frac{P}{2} \cdot \mathrm{Re}[(\underline{\psi}_{q+})^* \underline{I}_{d+} - (\underline{\psi}_{d+})^* \underline{I}_{q+}] \\ T_{(cage)-} &= \frac{P}{2} \cdot [\mathrm{Re}(\underline{\psi}_{q-})^* \underline{I}_{d-} - (\underline{\psi}_{d-})^* \underline{I}_{q-}] \\ \therefore T_{avg} &= T_{(cage)+} + T_{(cage)-} \end{aligned} \tag{5}$$

$$T_m = \frac{P}{2} \cdot \left[\frac{1}{\beta} \cdot \psi_{dm} I_{qm} - \beta \cdot \psi_{qm} I_{dm} \right] \tag{6}$$

The average air-gap resultant electromagnetic torque is given by (7), and Fig. 4 shows each torque and starting capacitor is off when the slip is 0.2

$$T_e = T_{avg} + T_m \tag{7}$$

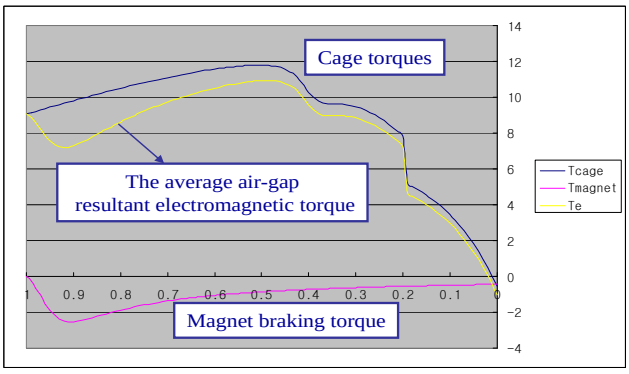

Fig. 4. The average air-gap resultant electromagnetic torque

III. Design And Analysis Result

Except for the shape of the conductor bars and the usage of PM, the stator and rotor size of prototype LSPM motor are the same compared with the single-phase induction motor. Compared to the induction motor, the efficiency of prototype LSPM motor is increased about 5% due to the loss reduction at the conductor bars, but the maximum torque is decreased about 12%. Therefore, this paper designs the LSPM motor improving the efficiency and maximum torque as compared with the induction motor.

The characteristic map obtained by the equivalent circuit shows the response of the efficiency and maximum torque according to the change of saliency ratio, back-EMF and d- and q-axis inductance and is given in Fig. 5. The d- and q-axis inductance is calculated under the constant current angle, and the maximum torque is estimated as follows:

$$T = P_n\left[\psi_a i_q + (L_d - L_q) i_d i_q\right] = T_m + T_r \quad (8)$$

The maximum torque is increased as back-EMF is great, and d-axis is decreased when the saliency ratio is constant. Therefore, the increase direction of the maximum torque is shown in Fig. 5 (a), (c) and (e).

The calculation of the efficiency is expressed as (9) and the core and mechanical loss are ignored.

$$Eff. = \frac{P_{out}}{P_{out} + P_{loss}} \times 100\ [\%] \quad (9)$$

Where, P_{out} is mechanical output and P_{loss} is the copper loss.

The efficiency is increased as back-EMF or d-axis inductance is great when the saliency ratio is constant. Thus, the increase direction of efficiency is shown in Fig. 5 (b), (c) and (f).

The region satisfying the efficiency and maximum torque as the saliency ratio is increased is expanded. As the saliency ratio grows, the maximum torque is increased, because the effect by the difference of d- and q-axis inductance is bigger than the effect by the decrease of iq. The region to satisfy the efficiency is expanded, because the copper loss is decreased by the reduction of iq. The design to satisfy both the efficiency and the maximum torque is difficult, because the increase direction of the efficiency and maximum torque is opposite. Therefore, in the initial design stage, the characteristic map is very important in order to determine the design direction. From the result of characteristic map, the efficiency of prototype LSPM motor satisfies the required efficiency, but the maximum torque is not. Therefore, back EMF and salient ratio to satisfy the characteristics of prototype LSPM motor should be enhanced.

The optimal design as regards the double-layer shape based on prototype LSPM motor is performed, because the region satisfying the characteristics due to the increase of saliency ratio is expanded, and design parameters are shown in Fig. 6.

The effects of design factors concerning back-EMF and saliency ratio obtained by DOE are shown in Fig. 7. Lpm1 and Gpm mainly affect the back-EMF and the saliency ratio, So RSM is firstly performed by the two design factors and the objective function and constraint condition are defined as follows:

- Objective function:

  Efficiency > 90 [%], Maximum torque > 130 [kgfcm]

- Subject to:

  Output > 2 [kW], starting torque > 26 [kgfcm]

RSM is secondly performed by PSpm, PM position in the layer 1 and layer 2, and Afb2, the angle of flux-barrier in layer 2.

Both the back-EMF and the salient ratio as shown in Fig. 8 are satisfied with the efficiency and maximum torque when Lpm1 and Gpm are 7.0 mm and 2.6 mm, and PSpm and Afb2 are 0 mm and 22.06o, respectively. The motor parameters of improved LSPM motor estimated by FEM are shown in table I and they are in the region of characteristic map satisfying the efficiency and the maximum torque.

The steady state characteristics are analyzed by FEM, and the relative comparisons between single phase induction motor, prototype LSPM motor and improved LSPM motor are shown in Fig. 9.

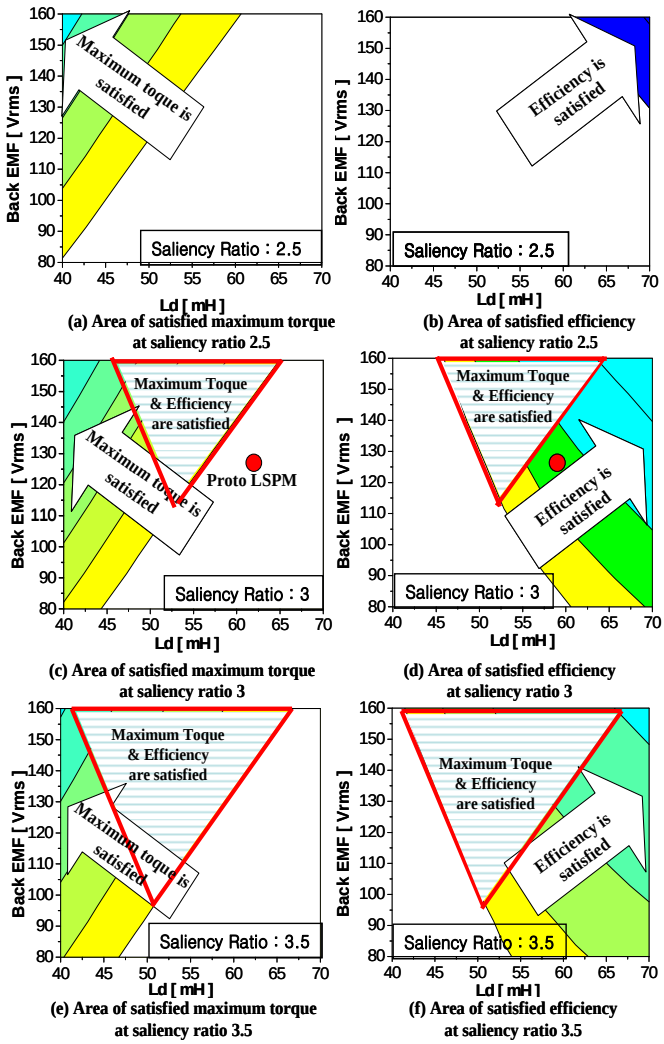

Fig. 5. Characteristic map

In comparison with the induction motor, the efficiency of improved LSPM motor is increased about 5% due to the reduction of conductor bar loss, and the synchronous speed is extended from 2867rpm to 3000rpm. The experimental results of single-phase induction motor, prototype LSPM motor and improved LSPM motor are shown in Fig. 10. From the comparison, the improved LSPM motor satisfies maximum torque and synchronous speed, and the efficiency is increased about 4.3% than the single-phase induction motor. Rotor and stator of improved LSPM motor is shown in Fig. 11.

IV. CONCLUSIONS

In this paper, the double-layer rotor structure design method to improve the characteristics of prototype LSPM motor is presented. The characteristics are investigated with the equivalent circuit according to the change of motor parameters. Moreover, the main design factors related to the characteristics are selected by DOE, and the optimal design is performed with them. In the end, the validity of the method is verified by test.

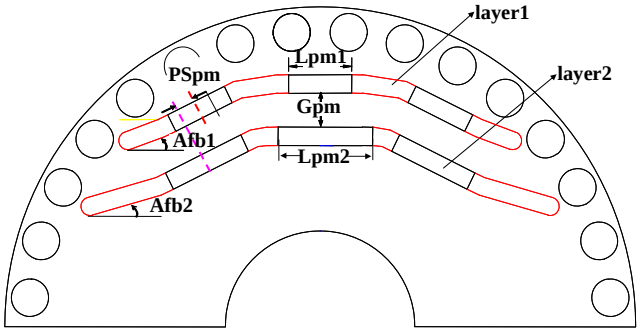

Fig. 6. Design parameter

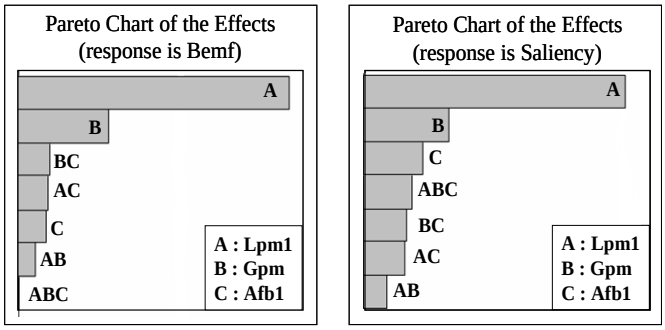

Fig. 7. Effect of design factor of back-EMF and saliency ratio

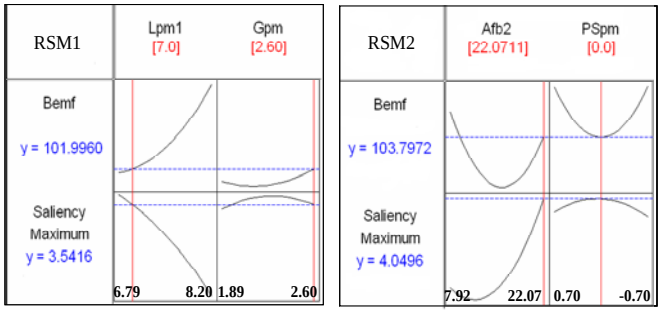

Fig. 8. Response surface of back-EMF and saliency ratio

TABLE I
COMPARISON OF MOTOR PARAMETERS

	Back EMF[Vrms]	Ld[mH]	Lq [mH]
Proto LSPM	125	63	186.48
Improved LSPM	103	53	187.62

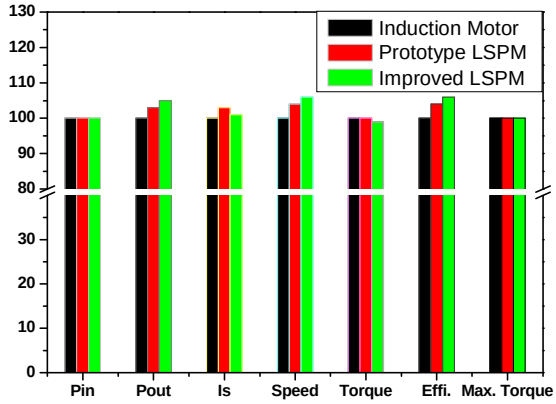

Fig. 10. Comparison of FEM results

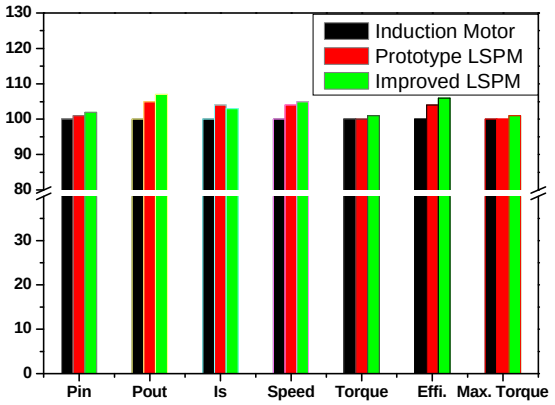

Fig. 11. Comparison of test results


Fig. 9. Rotor and stator of improved LSPM motor

REFERENCES

[1] T. J. E. Miller, "Single-phase permanent magnet motor analysis," IEEE Trans.Ind. Applicat., no. 4, pp. 651-658, 1985.

[2] H. Nam, K. H. Ha, J. J. Lee, J. P. Hong, and G. H. Kang, "A study on iron loss analysis method considering the harmonics of the flux density waveform using iron loss curves tested on Epstein samples," IEEE Trans. Magn., vol. 39, pp. 1472–1475, May 2003.

[3] Mircea Popescu, Senior Member, IEEE, T. J. E. Miller, Fellow, IEEE, "Asynchronous Performance Analysis of a Single-Phase Capacitor-Start, Capacitor-Run Permanent Magnet Motor", IEEE Trans. On Energy covers. vol. 20, NO. 1, March 2005.

[4] G. H. Kang, J. Hur, H. Nam, J. P. Hong, and G. T. Kim, "Analysis of irreversible magnet demagnetization in line-start motors based on the finite-element method," *IEEE Trans.* vol. 39, NO. 3, pp. 1488-1491, May 2003.